In-situ temperature monitoring of an internal insulated wall in a historic building

Kristian Hutkai[1*], *Dusan* Katunsky[1], and *Richard* Balaz[2]

[1]Technical university of Kosice, Faculty of Civil Engineering, Institute of Architectural Engineering, Vysokoškolská 4, 042 00 Kosice, Slovakia
[2]Technical university of Kosice, Faculty of Civil Engineering, Expert´s Institute in Construction, Vysokoškolská 4, 042 00 Kosice, Slovakia

Abstract.. The subject of the contribution is the evaluation of in-situ monitoring of an internally insulated wall in a historical building in Levoča. The paper compares the development of surface temperatures, temperatures under the thermal insulation and temperatures in the masonry at a depth of 100 mm when using calcium silicate board and phenolic foam. The temperatures of the insulated walls are compared with the reference temperatures of the uninsulated wall. As part of the measurements, the parameters of the internal environment are also monitored. The aim of the contribution is to quantify the effect of internal insulation on the development of temperatures in the perimeter structure and its effect on the quality of the internal environment.

1 Introduction

The aim of the energy-efficient building concept is to establish a collection of buildings characterized by high energy efficiency and a minimal carbon footprint. In this context, the thermo-physical attributes of the building elements employed serve as pivotal considerations during the architectural planning phase [1]. The determination of thermal characteristics associated with building structures often presents challenges, particularly in the case of existing historic edifices and artifacts imbued with significant historical heritage. Such constructions frequently exhibit technological intricacy, and their materials may manifest varying levels of degradation [2–4]. Studies since the 1990s have found that there is a difference between actual and simulated energy efficiency [5–9], as well as between measured and calculated thermal properties of building elements [3,10–16]. The primary factors contributing to these discrepancies are commonly linked to user behaviors and activities, material alterations, building aging, structural flaws, technological effectiveness, and building operation and maintenance practices [3,7,17–19]. In-situ measurements have emerged as invaluable tools for assessing the actual thermal performance of building elements within existing structures. This is because values obtained directly on-site under real conditions can diverge significantly from theoretical projections, potentially influencing the overall evaluation of the building. Employing laboratory methods in existing

* Corresponding author: kristian.hutkai@tuke.sk

structures can often be laborious and financially burdensome, and for historically preserved buildings, their application may pose significant challenges or even be impractical [20].
In situ measurement provides a unique possibility of monitoring quantities that laboratory measurements cannot clearly replicate. While laboratory measurements provide accurate measurements under controlled boundary conditions, they often fail to reveal the complexities and nuances of real-world conditions. In-situ measurements are performed directly at the site of the given structure, which has specific boundary conditions characteristic of the given surroundings, which represents a more accurate representation of the investigated system. In-situ measurement gives immediate feedback, thanks to which it is possible to react almost immediately to unexpected changes or events. This ability to monitor in real time is especially valuable when monitoring building structures that are exposed to conditions that change over time, even in unpredictable ways - rain, wind, sudden cooling of the air or solar radiation.

2 Methodology

Experimental temperature measurement will take place in a historical building in Levoča, which is in active operation as a social service center and is located in the historic center of the city. The monitored perimeter structure is made of solid burnt bricks on cement mortar. The total thickness of the structure is 550 mm, including the plaster system with a thickness of 20 mm from the interior and from the exterior, and it is located on the 1st floor. The wall is oriented to the north, in which the structure is exposed to the most adverse weather conditions, when it is the most hypothermic, the least exposed to the sun's rays, and in which the disturbances associated with heat-humidity processes occur most often. Material characteristics are shown in tab. 1 based on STN 73 0540-3 [21].

Table 1. Material characteristics of the perimeter structure.

Layer	d (m)	λ (W/m.K)	c (J/kg.K)	ρ (kg/m^3)	μ (-)	R (m^2.K/W)
Exterior render	0.02	0.99	790	2000	19	0.020
Solid brick	0.5	0.88	900	1800	9	0.568
Interior render	0.02	0.88	790	2000	19	0.034
						0.802

During the experiment, two thermal insulation systems with different structural and physical behavior will be investigated. Diffusion open, capillary active system with calcium silicate board and vapor barrier system using phenolic foam with vapor barrier layer.

The subject of the analysis are the temperatures in individual parts of the perimeter structure. The thermal resistance of the structure R (m^2.K/W) is an evaluation parameter when monitoring the temperature in different parts of the structure. For this reason, the thickness of the calcium-silicate board was chosen to be 100mm with a total thermal resistance of 3.011 and a thickness of phenolic foam of 50mm with additional layers of vapor barrier layer and plasterboard cladding with a total thickness of 62.5mm with a thermal resistance of 3.260. In table 2.-3. the thermal-technical parameters of the monitored insulated compositions are shown.

Table 2. Material characteristics of the perimeter structure with calcium-silicate board

Layer	d (m)	λ (W/m.K)	c (J/kg.K)	ρ (kg/m^3)	μ (-)	R (m^2.K/W)
Exterior render	0.02	0.99	790	2000	19	0.020
Solid brick	0.5	0.88	900	1800	9	0.568
Interior render	0.02	0.88	790	2000	19	0.034
Adhesive mortar	0.005	0.2		800	1	0.025
CaSi board	0.1	0.043	850	115	3	2.325
Adhesive mortar	0.005	0.2		800	1	0.025
						3.011

Table 3. Material characteristics of the perimeter structure with fenolic foam

Layer	d (m)	λ (W/m.K)	c (J/kg.K)	ρ (kg/m^3)	μ (-)	R (m^2.K/W)
Exterior render	0.02	0.99	790	2000	19	0020
Solid brick	0.5	0.88	900	1800	9	0.568
Interior render	0.02	0.88	790	2000	19	0.034
Air layer	0.04	0.23	1000	1,3	0.38	0.174
Phenolic foam	0.05	0.021	1400	35	35	2.381
Vapor barrier	0.001	2.3	2300	130	20000	0
Gypsum board	0.0125	0.15	1090	750	9	0.083
						3,26

2.1 Monitoring devices

Instrumentation from the monitoring infrastructure of the Faculty of Civil Engineering, which has already been used in various research tasks, is used to monitor selected quantities. NTC N type resistance sensors with a measurement range of -50 to 100 ˚ C with a resolution of hundredths of a degree and with an accuracy of ±0.05 ˚ C are used to measure the temperature at a depth of 100 mm in the masonry. To monitor the temperature at the interfaces of the masonry and thermal insulation and to monitor surface temperatures, NiCr-Ni (K) thermocouples with a resolution of tenths of a degree are used, which cover the measurement range from -200 to +1370˚ C. The parameters of the internal and external environment, such as temperature and relative humidity, are monitored using digital sensors FHAD46-C with a decimal by resolution. The measurement range is -20 to +60˚ C and 5-98%. The linear accuracy of these sensors is ±1.8% in the range of 20-80% at 25˚ C. The acquisition of data from the sensors takes place through the fully automatic measuring device ALMEMO 5690-1, which is connected to a computer using a LAN network cable (to the measuring center). The data is recorded in minute intervals and stored in an external storage from which the measured values are manually exported to the .xls format, or csv. Temperature sensors were installed in two horizontal and two vertical axes in the plane of the perimeter wall. The lower horizontal axis is located at a height of 850 mm and the higher axis at a height of 2650 mm above the floor level of the room. The vertical axes are located 500 mm from the window structure. The same number of sensors are placed in each axis. NTC resistance sensors were placed in the masonry at a depth of 100 mm, NiCr-Ni

thermocouples were placed under the thermal insulation (on the surface of the masonry itself) and on the inner surface of the entire wall structure. In the case of the unheated reference sample, the temperature at a depth of 100 mm and the surface temperature were monitored. On October 25, 2023, the long-term monitoring of the internally insulated historic perimeter structure began in full measuring equipment. Data recording took place with a measuring step of 1 minute.

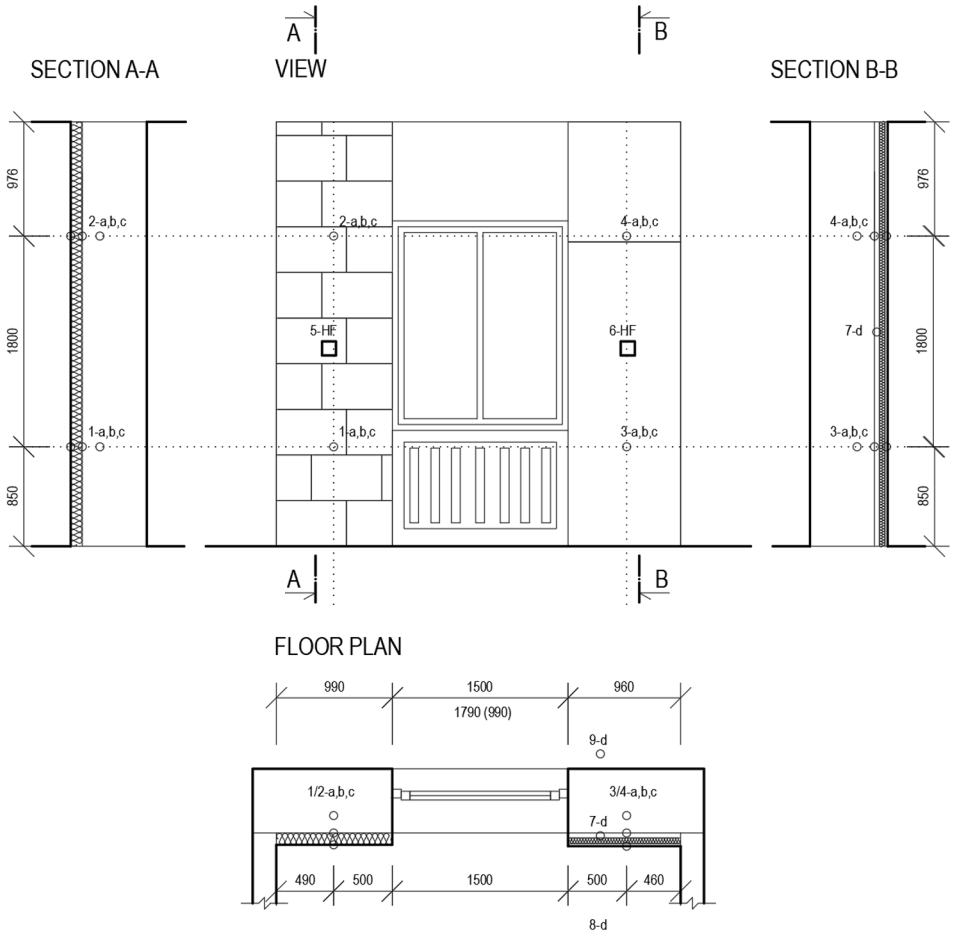

Fig.1. Location of sensors on monitored samples

Figure 2 shows temperature trends at a depth of 100mm in the masonry during the period 25.10.2023 to 10.3.2024. The initial temperature difference between the insulated and the reference sample on the day of the start of the experiment at altitude is caused by the time lag between the completion of the assembly work and the start of data collection. Approximately two months after installation, on 25/10/2024, it is possible to observe a difference in the initial temperature at a depth of 100mm in the masonry of 4.5˚ C. In the context of external temperatures in the relatively warm months – September and October, the difference of 3˚ C appears to be fundamental, which subsequently, it gradually increases during the monitoring period. On the day of the start of monitoring, the building was already fully heated and the temperature development clearly shows the dicrease temperature of the masonry due to the presence of heat-insulating materials. The monitored temperatures at two

heights for heated samples approximately coincide. A slightly higher temperature is recorded by the lower sensor with phenolic foam. During assembly, the presence of heating distributions was poorly evaluated and the lower edge of the phenolic foam was not finished in such a quality that would prevent the influence of heat radiation from the pipe. This means that the lower sensor was affected by the distribution of the hot water supply pipe and, until the fault was removed, showed a higher temperature on average of 1.99 ˚ C. After discovering the undesirable effect, on 12/02/2024, modifications were made to the composition, when aluminum tape was used on the lower edge of the composition and thermal insulation was applied to the pipe of the supply pipe of the heating element.

Due to approximately the same thermal resistance of the heated samples, the development of temperatures is approximately identical. The lowest temperature was recorded at the upper position of the phenolic foam sensor with a temperature of 2.35 ˚ C at an outside temperature of -13.46 ˚ C on 11.1.2024. At the same time, the upper sensor with the calcium silicate board recorded the lowest temperature of 2.7 ˚ C and the lower sensor with the temperature of 3.49 ˚ C. The recorded temperature of the lower sensor with the phenolic foam is 5.13 ˚ C.

In the case of the reference, non-insulated wall, the temperature trends reach higher values on average by approximately 8 ˚ C than in the case of insulated ones. The initial temperature on 25/10/2023 is 18.79 ˚ C and by the beginning of December it gradually decreases to approximately 16 degrees. During December, the temperature oscillates at the level of 15 ˚ C to 17 ˚ C. At the beginning of January, when the outside temperature drops sharply, the temperature drops to the level of 12.88 ˚ C. Since then, with the gradual warming of the external environment, the temperature course at a depth of 100 mm has a rising character. At the beginning of the measurement period, a large temperature fluctuation can be seen at the lower measuring point of the unheated sample due to a poorly attached sensor. Due to the low-quality tape and after peeling off the sensor, it practically recorded the temperature of the surrounding air. After the correction of the error on 28.12.2023, the temperature course of the lower sensor has a similar character as in the case of the upper one. Since then, an average deviation of 1.08 ˚ C can be observed.

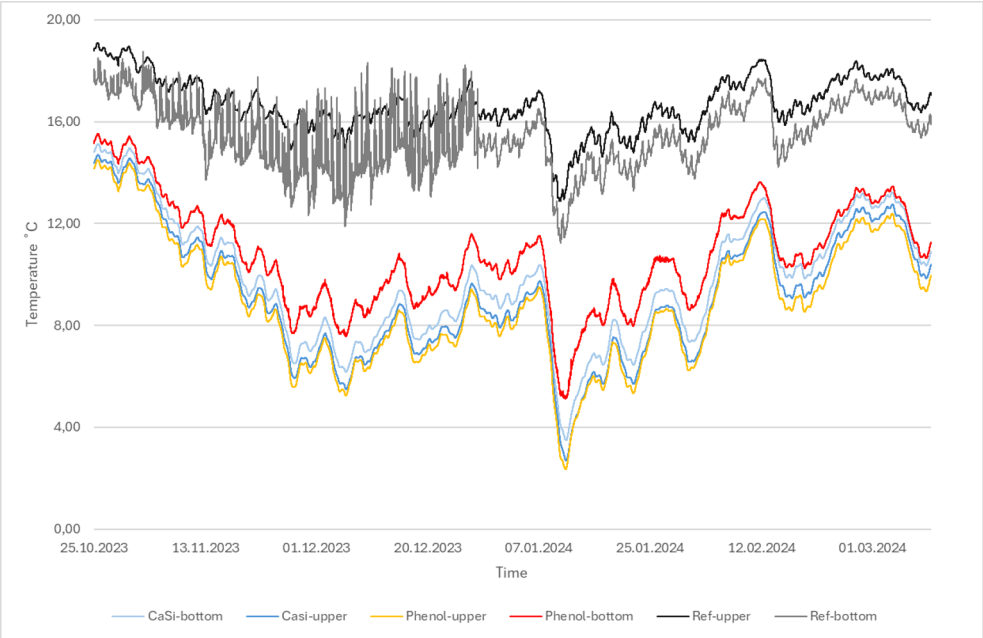

Fig.2. The course of temperatures in the masonry depth of 100 mm.

In fig. 3 we can see the course of surface temperatures. During the first two months of measurement, in addition to the high fluctuation of the surface temperature of the reference sample, it is also possible to observe the surface temperature approximately the same as the air temperature of the room. During the inspection on 28/12/2023, it was found that the thermocouples monitoring the surface temperatures of the reference sample were unglued and were recording the air temperature. After correcting the error, from 29.12.2023 you can see the actual measured surface temperatures for each sample. The lowest surface temperature for the reference sample of 15.7 ˚ C is reached at the bottom position of the sensor on 15/02/2024. At the same time, a temperature of 19.2˚ C was recorded at the top position of the sensor. The 3.5˚ C temperature difference is probably caused by room ventilation, when the lower sensor, closer to the window, could have been affected by the cold outside air. The highest surface temperature of the reference sample is reached on 4/2/2024 with a temperature of 21.0 and 20.9 ˚C. During the monitored period, the average temperature difference between the lower and upper position of the sensor was 0.5 ˚ C. In heated samples, the lowest temperatures are recorded on 31.1.2024. In the case of a calcium-silicate board, the lowest temperature is 18.7 ˚ C in the upper position and 17.3 ˚ C in the lower position. The highest temperatures are recorded at 23.8 and 23.9 ˚ C. The average temperature is 22.5 ˚ C. For phenolic foam, the lowest temperature is 16.6 ˚ C at the top position and 18.5 ˚ C at the bottom. The highest temperatures are recorded at 23.9 and 23.7 ˚C. The average surface temperature of the phenolic foam during the monitoring period is 22.4 ˚C.

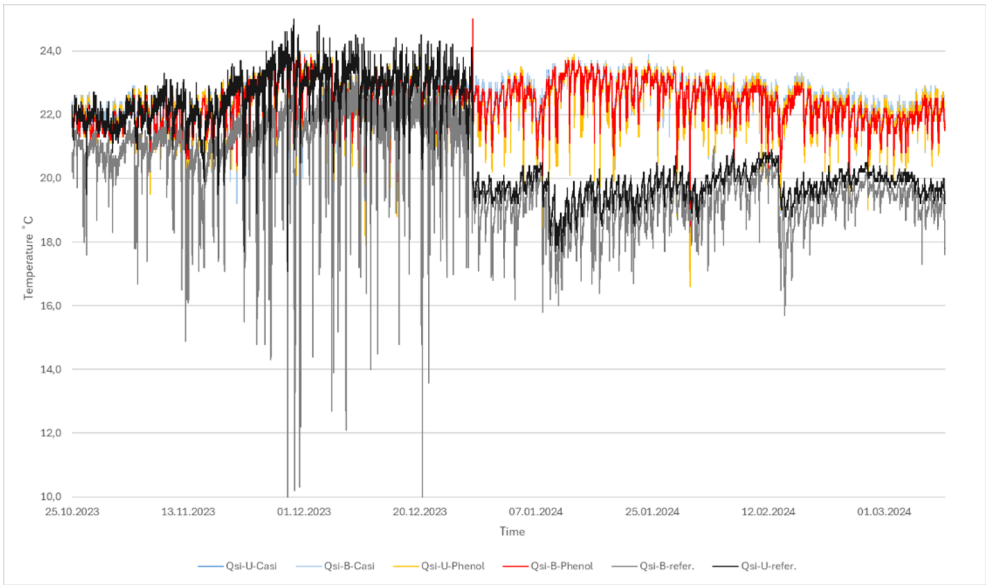

Fig.3. The course of surface temperatures.

Conclusion

The goal of the in-situ measurements was to determine the actual thermal-technical behaviour of the internally insulated historical wall, on the basis of which it will be possible to create a numerical model. In addition to examining the temperatures of the reference wall, the temperature courses of two insulated samples of the perimeter masonry were also monitored. The selected thermal insulation materials and the thermal insulation systems created with

them are declared by their manufacturers as a suitable solution for the purpose of reducing the energy demand of historic buildings. The application of thermal insulation on the inner surface of the perimeter structure has a clearly positive effect in terms of the course of surface temperatures. Heated samples have an average temperature of approximately 3.5 ˚ C higher than non-heated ones. This difference has a significantly positive effect on the internal thermal comfort for the occupants of the room. Thermal comfort is an important indicator of the quality (microclimate) of the room, especially in the case of people with disabilities. Temperatures at a depth of 100 mm in the case of insulated samples are lower than insulated ones by approximately 7.5 ˚ C. This means decreased temperature of the perimeter masonry, the consequence of which may be malfunctions associated with frost if the temperature drops below 0 ˚ C. During the monitored period in this part of the masonry no minus temperature was recorded. The temperature at a depth of 100 mm of the non-insulated sample decreased by 2.84 ˚ C on average compared to the surface temperatures. In the case of insulated samples, the temperature drop is 13.4 ˚ C. In-situ monitoring of the insulated wall was used for a partial analysis of the effect of thermal insulation applied to the internal surface in the context of the course of temperatures on or in structures during the heated period. Based on the obtained data, it is possible to create a simulation model, with the help of which it will be possible to monitor aspects of internal insulation in the context of temperature development and water accumulation in the perimeter wall.

This research is supported by VEGA 1/0626/22 Design and evaluation of building structures and the indoor environment of buildings for demanding conditions.

References

1. Directive (EU), 2018/844 of the European Parliament and of the Council of 30 may 2018 amending Directive 2010/31/EU on the energy performance of buildings and Directive 2012/27/EU on energy efficiency, Off. J. Eur. Union (2018).
2. P. Biddulph, V. Gori, C.A. Elwell, C. Scott, C. Rye, R. Lowe, T. Oreszczyn, *Inferring the thermal resistance and effective thermal mass of a wall using frequent temperature and heat flux measurements*, Energy Build. **78** (0) (2014) 10–16 http://dx.doi.org/10.1016/j.enbuild.2014.04.004.
3. E. Lucchi, *Thermal transmittance of historical brick masonries: a comparison among standard data, analytical calculation procedures, and in situ heat flow meter measurements,* Energy Build. **134** (2017) 171–184 https://doi.org/ 10.1016/j.enbuild.2016.10.045.
4. E. Lucchi, *Thermal transmittance of historical stone masonries: a comparison among standard, calculated and measured data*, Energy Build. **151** (2017) 393–405 https://doi.org/10.1016/j.enbuild.2017.07.002.
5. E. Burman, D. Mumovic, J. Kimpian, *Towards measurement and verification of energy performance under the framework of the European directive for energy performance of buildings*, Energy **77** (2014) 153–163 https://doi.org/ 10.1016/j.energy.2014.05.102.
6. D. Majcen, L. Itard, H. Visscher, *Actual and theoretical gas consumption in Dutch dwellings: what causes the differences?* Energy Policy **61** (2013) 460– 471 https://doi.org/10.1016/j.enpol.2013.06.018.
7. P. de Wilde, *The gap between predicted and measured energy performance of buildings: a framework for investigation*, Autom. Constr. **41** (2014) 40–49 https://doi.org/10.1016/j.autcon.2014.02.009.
8. M. Sunikka-Blank, R. Galvin, *Introducing the prebound effect: the gap between performance and actual energy consumption*, Build. Res. Inf. **40** (3) (2012) 260–273.

9. D. Majcen, L.C.M. Itard, H. Visscher, *Theoretical vs. actual energy consumption of labelled dwellings in the Netherlands: discrepancies and policy implications*, Energy Policy **54** (2013) 125–136 https://doi.org/10.1016/j.enpol.2012. 11.008.
10. Thermal Insulation – Building Elements – In-Situ Measurement of Thermal Resistance and Thermal Transmittance – Part 1: Heat Flow Meter Method (ISO 9869-1:2014).
11. R. Albatici, A.M. Tonelli, M. Chiogna, *A comprehensive experimental approach for the validation of quantitative infrared thermography in the evaluation of building thermal transmittance*, Appl. Energy **141** (0) (2015) 218–228 http: //dx.doi.org/10.1016/j.apenergy.2014.12.035.
12. G. Desogus, S. Mura, R. Ricciu, *Comparing different approaches to in situ measurement of building components thermal resistance*, Energy Build. **43** (10) (2011) 2613–2620 https://doi.org/10.1016/j.enbuild.2011.05.025.
13. F. Asdrubali, F. D'Alessandro, G. Baldinelli, F. Bianchi, *Evaluating in situ thermal transmittance of green buildings masonries—a case study*, Case Stud. Constr. Mater. **1** (0) (2014) 53–59 http://dx.doi.org/10.1016/j.cscm.2014.04. 004.
14. L. Evangelisti, C. Guattari, P. Gori, R. Vollaro, *In situ thermal transmittance measurements for investigating differences between wall models and actual building performance*, Sustainability **7** (8) (2015) 10388 https://doi.org/10. 3390/su70810388.
15. K. Gaspar, M. Casals, M. Gangolells, *A comparison of standardized calculation methods for in situ measurements of façades U-value*, Energy Build. **130** (2016) 592–599 https://doi.org/10.1016/j.enbuild.2016.08.072.
16. L. Evangelisti, C. Guattari, F. Asdrubali, *Influence of heating systems on thermal transmittance evaluations: simulations, experimental measurements and data post-processing*, Energy Build. **168** (2018) 180–190 https://doi.org/10. 1016/j.enbuild.2018.03.032.
17. E. Cuerda, O. Guerra-Santin, F.J. Neila, N. Romero, *Evaluation and comparison of building performance in use through on-site monitoring and simulation modelling*, in: Proceedings of the 3rd IBPSA-England Conference BSO 2016, Great North Museum, Newcastle, 2016.
18. V. Gori, V. Marincioni, P. Biddulph, C.A. Elwell, *Inferring the thermal resistance and effective thermal mass distribution of a wall from in situ measurements to characterise heat transfer at both the interior and exterior surfaces*, Energy Build. **135** (2017) 398–409 https://doi.org/10.1016/j.enbuild. 2016.10.043.
19. J. Bros-Williamson, C. Garnier, J.I. Currie, *A longitudinal building fabric and energy performance analysis of two homes built to different energy principles*, Energy Build. **130** (2016) 578–591 https://doi.org/10.1016/j.enbuild.2016. 08.052.
20. Ž. Koški, I. Ištoka, I. Milicevi ˇ c´, *Klasifikacija elemenata zgrada u funkciji mjerenja zrakopropusnosti*, Grad¯evinar **65** (2013).
21. STN 73 0540-3 : 2013, Tepelná ochrana budov. Tepelnotechnické vlastnosti stavebných konštrukcií a budov - Časť 3: Vlastnosti prostredia a stavebných výrobkov.